

A&A 381, 401–407 (2002)
 DOI: 10.1051/0004-6361:20011579
 © ESO 2002

**Astronomy
&
Astrophysics**

A 327 MHz VLBI study of high redshift radio galaxies 1345+245, 1809+407 and 2349+289

Z. Cai^{1,2}, R. Nan¹, R. T. Schilizzi^{2,3}, G. K. Miley³, M. A. R. Bremer⁴, B. van Dam³, H. J. A. Röttgering³,
 H. Liang^{5,2}, K. C. Chambers⁶, L. I. Gurvits², and H. Y. Zhang¹

¹ Beijing Astronomical Observatory, National Astronomical Observatories, CAS, 20 Datun Road,
 Chaoyang District, Beijing 100012, PR China

² Joint Institute for VLBI in Europe, PO Box 2, 7990 AA Dwingeloo, The Netherlands

³ Leiden Observatory, PO Box 9513, 2300 RA Leiden, The Netherlands

⁴ Space Research Organization of the Netherlands, Sorbonnelaan 2, 3584 CA Utrecht, The Netherlands

⁵ Shanghai Astronomical Observatory, Shanghai 200030, PR China

⁶ Institute for Astronomy, University of Hawaii, 2680 Woodlawn Rd., Honolulu, HI 96822, USA

Received 2 May 2001/ Accepted 18 October 2001

Abstract. Three high redshift radio galaxies, 1345+245 (4C 24.28, $z = 2.889$), 1809+407 (4C 40.36, $z = 2.267$) and 2349+289 (4C 28.58, $z = 2.905$) were observed with VLBI at 327 MHz giving an angular resolution of $\simeq 40$ –100 mas and yielding images with the off-source noise level of $3\sigma \simeq 3.5$ mJy/beam. On the centiarcsecond scale, the three sources are each characterized by two components with asymmetry both in flux density and in size. The compact components in the VLBI maps correspond to the hot spots in the VLA maps. No radio cores have been detected. The physical parameters for the components derived are consistent with a model in which shocks accelerate electrons in the hotspots.

Key words. galaxies: high redshift – galaxies: magnetic fields – galaxies: jets

1. Introduction

The most distant radio sources and their parent galaxies provide powerful probes of the early Universe. They give an opportunity to identify and study massive galaxies in the “galaxy formation” period in the redshift range $2 \lesssim z \lesssim 6$ (for a review see McCarthy 1993; Röttgering et al. 1996), when most galaxy formation is believed to have taken place.

Three components of the observable emission of radio galaxies, IR–optical–UV continuum, optical emission lines and radio continuum, are all highly luminous and spatially extended. Not only can different diagnostics be derived for each of these, but studies of the relationships between them can place unique constraints on the emission mechanisms, the dynamical state of the thermal plasma, the physical state of the galactic environment and the star formation history.

Unlike the situation for nearby radio galaxies, the radio emission of $z \gtrsim 0.6$ radio galaxies is in most cases roughly aligned with the optical/IR continuum (Chambers et al. 1987; McCarthy et al. 1987). Many models have been proposed or considered to account for the alignment

effect (e.g. see Chambers & Miley 1990; McCarthy 1993; Röttgering & Miley 1996), but none of them are entirely satisfactory. Currently it seems that three physical mechanisms contribute to the alignment effect, each with a relative strength varying from object to object: (i) scattering of light from a hidden quasar by electrons or dust (Tadhunter et al. 1989; Fabian 1989), (ii) star formation induced by the radio jet (Chambers et al. 1987; McCarthy et al. 1987; De Young 1989; Rees 1989; Begelman & Cioffi 1989) and (iii) nebular continuum emission from the emission line gas (Dickson et al. 1995).

One of the most powerful methods of studying the nature of these objects and constraining models of the alignment effect is to investigate the radio and optical morphology at higher angular resolution. We are carrying out a programme to study the radio emission from high redshift radio galaxies using VLBI. The programme has four main aims:

1) to investigate substructure in the radio hotspots observed by the VLA. Any substructure may be related to shocks induced by a radio jet;

2) to image sub-arcsecond structure in the nuclei of the high redshift galaxies at the highest available angular resolutions and allow detailed comparison with the HST optical images;

Table 1. VLBI telescopes and their characteristics at $\lambda = 92$ cm (327 MHz).

Station	Diameter (m)	T_{sys} (K)	Sensitivity (K/Jy)
Green Bank	43	65	0.27
Jodrell Bank	76	100	1.10
OVRO	40	250	0.24
Simeiz	22	200	0.07
WSRT ^a	80	160	1.68
VLA ^a	115	100	2.08

^a WSRT and VLA were used in phased array mode; an equivalent diameter is given.

3) to compare the compact structures of high redshift galaxies with those of their high redshift quasars counterparts. This bears on questions of unification of quasars and galaxies;

4) to compare the compact nuclear radio structure of high redshift galaxies with those at low redshift to search for evolution in the morphological properties with redshift.

In this paper we present the first results from this project. We have carried out 92 cm (327 MHz) VLBI observations of nine high redshift galaxies selected from a list observed at 2 cm with the VLA and showing evidence of compact structure on scales of $0''.2$ (Chambers et al. 1996). The observations were conducted with a global network of telescopes. Fringes were detected from three of the nine objects, 1345+245, 1809+407 and 2349+289. The resulting images indicate that these objects have sub-structures on angular scales of $\simeq 50$ –100 mas.

2. Observations and data reduction

The sample of the radio galaxies included nine objects: 0124+495 (4C 49.06), 0508+605 (4C 60.07, $z = 3.791$), 0630+469 (4C 46.12), 0647+416 (4C 41.17, $z = 3.800$), 1345+245 (4C 24.28, $z = 2.889$), 1803+110 (3C 368, $z = 1.132$), 1809+407 (4C 40.36, $z = 2.267$), 2105+233 (4C 23.56, $z = 2.479$) and 2349+289 (4C 28.58, $z = 2.905$). They all have either known or suspected (0124+495 and 0630+469) high redshifts due to their very steep radio spectra. Observations of these objects were made at 92 cm with the telescopes listed in Table 1 on 9 June 1989. In addition, Iowa, Maryland Point, Ooty and Torun took part in the observations, but unfortunately, no usable data were produced for various reasons. Forty eight hours of snapshot observations were made with each source being observed for a total of about four hours split into 30 min scans at 7 or 8 different hour angles.

The signals were recorded using the standard Mk2 VLBI system with an effective bandwidth of 1.8 MHz (Clark 1973). The correlation was carried out on the Caltech Block 2 correlator, followed by global fringe fitting, calibration, imaging and model fitting using AIPS

(Cotton 1995; Diamond 1995; Walker 1995) and the Caltech VLBI package (Pearson 1991).

Fringe fitting for each data set was carried out separately. After averaging and editing, only the data from Jodrell Bank, Green Bank, OVRO, Simeiz, VLA and WSRT were kept. Poor signal to noise ratio forced us to eliminate data from Maryland Point, as well as the transatlantic data. In one case, 2349+289, the data from Simeiz were deleted in view of the unacceptably high correlated flux densities on all baselines. The reason for this is unknown.

Model fitting was carried out as the first step in the imaging process. For 1345+245 and 1809+407, data from Jodrell Bank, Simeiz and WSRT were used for this. For 2349+289, only the WSRT – Jodrell Bank baseline was used for model fitting. After an acceptable fit was achieved (usually, $\chi^2 < 3$), the phase corrected data were exported to AIPS for further imaging using the task “MX” with a large field and multi-windowing for the CLEAN procedure. The real observed beams for 1345+245, 1809+407 and 2349+289 are 102×85 mas (position angle -30 degree), 90×40 mas (position angle 10 degree) and 80×50 mas (position angle 25 degree), while the restore beams of the images are 100×100 mas.

3. Results

Table 2 gives the measured and calculated parameters for the three observed high redshift radio galaxies at 92 cm, and the radio spectra of the individual components of each source are displayed in Fig. 1 (Chambers et al. 1996).

3.1. Comments on individual sources

3.1.1. 1345+245

The source 1345+245 (4C 24.28, $z = 2.889$) has been imaged with the VLA in A-configuration at 20 and 6 cm, in B-configuration at 6 and 2 cm and in C-configuration at 2 cm (Chambers et al. 1996). Based on VLA imaging at several frequencies, it was classified by Carilli et al. (1997) as a compact steep spectrum (CSS) source. In the VLA images at 6 and 2 cm (resolution of $\simeq 400$ mas), 1345+245 consists of two radio lobes and a weak feature close to the eastern lobe B. The two lobes are asymmetric in flux density. The eastern lobe is more polarized than the western one, up to 12% at 2 cm, while the western lobe has the steeper spectrum. The weak feature has a steep spectrum and is believed to be a jet. The magnetic field in the source is directed at an angle of 45° to the line connecting the components A and B. The rotation measure is estimated to be ~ -35 rad m^{-2} .

The HST image of the source by Pentericci et al. (1999) shows a remarkable alignment of optical and radio structures along what is supposed to be a jet. This alignment is suggested to be a result of star formation triggered by the passage of the radio jet. Alternative mechanisms for

Table 2. Parameters of the observed sources and their images.

Source	z^a	RA (2000) ^b hh mm ss	Dec (2000) ^b dd ' "	Ang. size ^c (mas)	PA (deg)	Lin. size ^d (kpc)	S_{92} (Jy)	α_{327}^{1465e}
1345+245	2.889	13 48 14.82	+24 15 51.6	2439	45	16.41	3.30 ^f	
A				302×112	35	2.03×0.75	1.89	-1.55
B				194×97	167	1.31×0.65	1.22	-0.85
1809+407	2.267	18 10 55.70	+40 45 23.6	3638	82	25.82	2.90 ^f	
A				175×142	128	1.24×1.01	1.97	-1.54
B				221×67	37	1.57×0.48	0.63	-0.48
2349+289	2.905	23 51 59.23	+29 10 29.0	14 497	-34	97.42	3.21 ^f	
A				88×61	9	0.50×0.41	1.92	-1.68
B				391×72	34	2.63×0.48	1.43	-1.97

^a Redshift from Chambers et al. (1996) and Chambers et al. (1988) for sources 1345+245, 1809+407 and 2349+289, respectively.

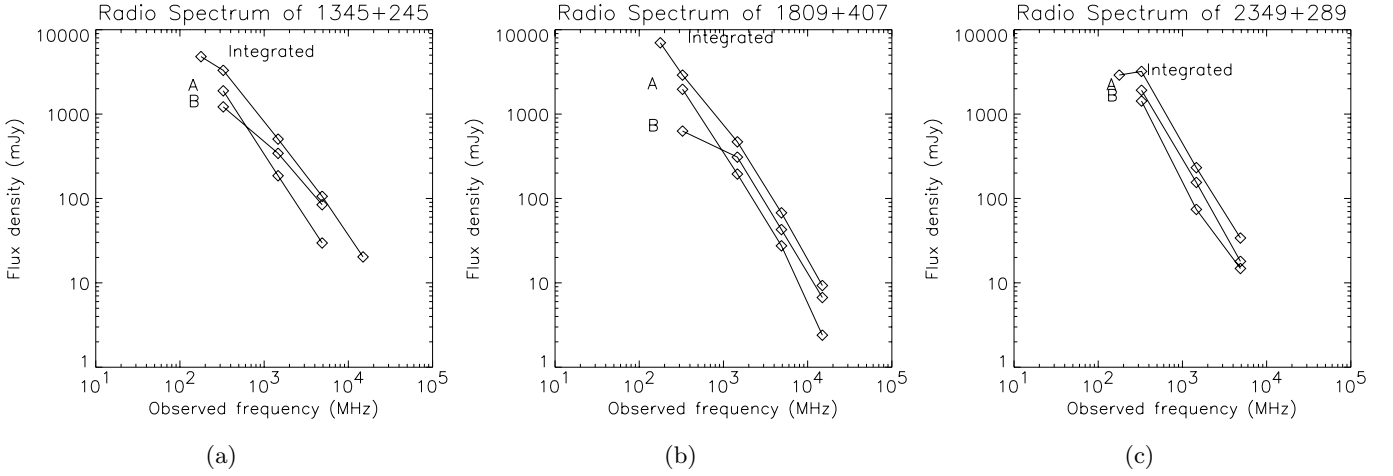
^b Coordinates correspond to a phase center as used for the data correlation and shown on the images (Figs. 2–4) as the frame origin.

^c Angular separation for the entire source or deconvolved angular sizes for components.

^d Corresponds to the angular separation/size (see footnote ^b). Here and throughout the paper we assume $H_0 = 65 \text{ km s}^{-1}/\text{Mpc}$ and $q_0 = 0.3$.

^e Spectral index values ($S \propto \nu^\alpha$) are calculated from flux densities at 1465 MHz (Chambers et al. 1996) and at 327 MHz (this paper).

^f VLA measurement, this work.

**Fig. 1.** Radio spectra of three sources: **a)** 1345+245, **b)** 1809+407, **c)** 2349+289. All the data have been published in Chambers et al. (1996).

the alignment in this source are discussed by Bremer et al. (1997).

The two components detected in our VLBI observation (Fig. 2) correspond to the lobes seen in the VLA maps by Chambers et al. (1996). The extended low-brightness structures in the VLA maps are completely resolved out in our observations, even on the shortest baseline WSRT – Jodrell Bank. The separation and orientation between the two components are in good agreement with those in the VLA maps. The two components are asymmetric in flux density and size. The western component A is stronger

than the eastern one, which is opposite to that seen in the VLA images at higher frequency (Fig. 1a). The two components show slightly elongated structures, both with position angles different from the line joining them. No emission has been detected at 92 cm at the position of the weak inner component visible in the VLA 6 and 2 cm map.

3.1.2. 1809+407

The radio galaxy 1809+407 (4C 40.36, $z = 2.267$) has been observed with the VLA at 20 cm (A-array), 6 cm

(B-array), 2 cm (C-array) and 90 cm (C-array) (Bremer 1991; Chambers et al. 1996). The 90 cm data allowed us to estimate the flux density only, due to the relatively low angular resolution of the measurement (Bremer 1991). The spectral index α_{178}^{1465} of the source is $\alpha \sim -1.28$ ($S \propto \nu^\alpha$) (Chambers et al. 1996). The source is remarkable due to its high degree of asymmetry in the radio polarization properties of the two lobes: the eastern lobe B is depolarised at all frequencies. The magnetic field is oriented at an angle of 45° to the jet direction and the rotation measure is about -45 rad m^{-2} . The spectral indices for both components are roughly the same ($\alpha_{1465}^{4885} \sim -1.63$).

Our 92 cm VLBI image (Fig. 3) has a similar morphology as the higher frequency VLA maps by Chambers et al. (1996). The extended low brightness regions in the VLA map have been almost completely resolved out. The western component A appears more compact, while only a small fraction of the low brightness emission in the eastern component has been detected. The ratio of flux density of the two components is ~ 3 which agrees with the estimate made from the variations of the visibility amplitude on the WSRT–Jodrell Bank baseline. The sum of flux densities of components A and B in our image ($\sim 2.60 \text{ Jy}$) accounts for about 90% of the total flux density of the source at 327 MHz. Figure 1b presents radio spectra of the components and the whole source.

3.1.3. 2349+289

The radio galaxy 2349+289 (4C 28.58, $z = 2.905$) is an edge-brightened FR II type object. VLA images (A-array at 20 and 6 cm and B-array at 6 cm) show that the source has two bright components roughly equal in brightness at both frequencies, but the eastern component B is fainter and has a somewhat steeper spectrum (Chambers et al. 1996). A flat-spectrum central component ($\alpha_{1465}^{4885} = -0.2$) is considered to be a core, which is not visible either in the 2 cm VLA map or in our VLBI map at 92 cm. The western component A shows an elongated jet-like structure. Both the western and the eastern components are polarized at roughly the same level (15%) in the VLA 6 cm image but differ in polarization percentage at 20 cm (Bremer 1991). The spectral indices of the western (A) and the eastern (B) components are $\alpha_{1465}^{4885} < -2.50$ and $\alpha_{1465}^{4885} < -2.32$ respectively (Chambers et al. 1996).

Near-infrared images obtained with the Keck I telescope by van Breugel et al. (1998) show an elongated structure and the maximum IR diameter is 3 arcsec, generally coinciding with the HST structure which shows a separation of 1 arcsec between the two bright rest-frame UV knots by Miley (1992). However, both optical and IR-structures are considerably smaller than the radio structure.

The magnetic field in both components is oriented at $\sim 45^\circ$ with respect to the main axis of the radio source, and the magnetic field strength in the western component A is larger than that in the eastern one. The rotation measure

is about -130 rad m^{-2} for the western component and -100 rad m^{-2} for the eastern one.

Our 92 cm image (Fig. 4) contains two components at the positions coinciding with those in VLA images. The separation between the two is $\sim 14.5 \text{ arcsec}$. The eastern component in the map is resolved at our resolution ($100 \times 100 \text{ mas}$); the angular sizes of its sub-components are smaller than 0.1 arcsec. Figure 1c presents the radio spectra of 2349+289 and its two components. The total flux density measurement at 102 MHz is 7.9 Jy (Dagkesamanskii et al. 2000), which suggests the total spectrum turns over at about 300 MHz.

3.2. Modeling the physical parameters

We modeled the physical parameters of the VLBI knots following Miley (1980) under the assumption of minimum energy conditions and energy equipartition. Table 3 lists the physical parameters of the observed radio emission (Table 2) of the three high redshift galaxies at 92 cm obtained under a set of “standard” assumptions (spectral cutoff frequencies $\nu_1 = 0.01 \text{ GHz}$, $\nu_2 = 100 \text{ GHz}$; ratio of heavy particles to electrons = 100; filling factor of the emitting regions = 1; the values of the major and minor axes are used to calculate the component sizes; and the angle between an assumed uniform magnetic field and the line of sight, $\phi = 90^\circ$).

The assumptions made for the ratio of heavy particles to electrons, the cut off frequencies (ν_1, ν_2), and the filling factor of the emitting area are highly uncertain. Moreover, we reconstruct the compact source structure only and miss the low brightness emission due to the sensitivity limitations and lack of short baselines in the VLBI observations, and this makes the calculations even less reliable. Another simplification is that we only consider the average effective magnetic field with orientation perpendicular to the line of sight. All these points suggest that we are attempting order of magnitude calculations only.

The magnetic field strengths (several times 10^{-3} G) in Col. 5 of Table 3 are significantly higher than typical nearby powerful radio galaxies (the value for Cygnus A is $\sim 3 \times 10^{-4} \text{ G}$, Carilli & Barthel 1996). At least in one more case of a high redshift galaxy the magnetic field is even stronger (4C41.17, $B_{\text{me}} \sim 1.5 \times 10^{-2} \text{ G}$, Gurvits et al. 1997). Neglecting the observational uncertainties, a possible reason may be that the density of the IGM and the intergalactic magnetic field in the distant universe is much higher than nearby, or alternatively, there has not been sufficient time for the magnetic field to lose energy and allow a diffuse magnetic field component to form in the IGM. We have also estimated physical parameters in the six components following the synchrotron self-absorption model proposed by Sligh (1963) (the slowly varying function of spectral index $K(\alpha) = 1$, spectral cutoff frequencies $f_1 = 100 \text{ MHz}$ and the values of the major axes of the components were chosen as the apparent angular diameter θ). The key value of both equipartition and self-absorption

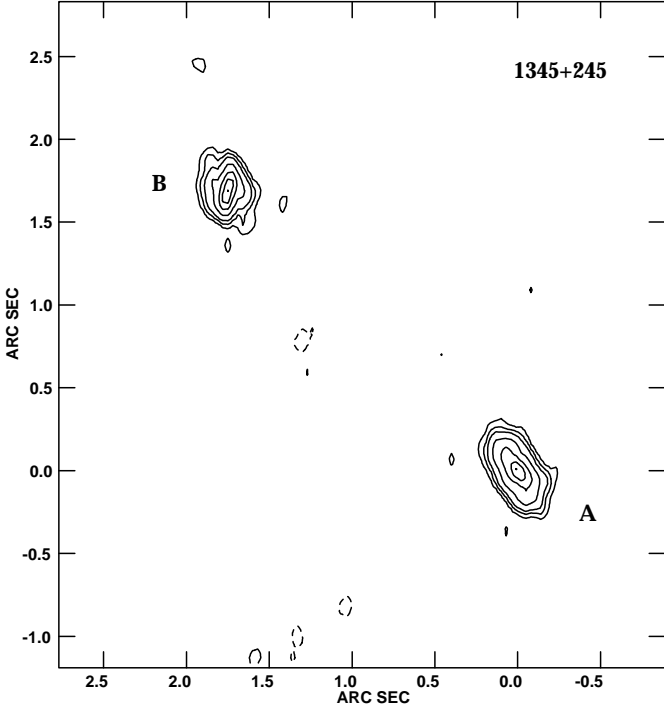


Fig. 2. Brightness distribution of the source 1345+245 at 327 MHz. Contours levels are $-2, 2, 5, 10, 25, 50, 75, 99\%$ of the peak flux density of 1.07 Jy/beam , beam size $100 \times 100 \text{ mas}$.

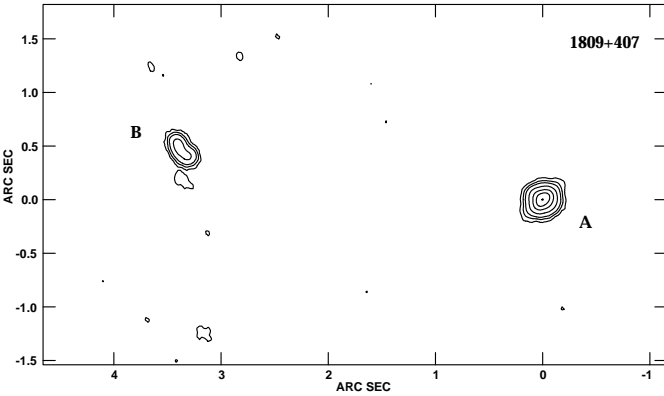


Fig. 3. Brightness distribution of the source 1809+407 at 327 MHz. Contours levels are $-2, 2, 3, 5, 10, 25, 50, 75, 99\%$ of the peak flux density of 0.621 Jy/beam , beam size is $100 \times 100 \text{ mas}$.

models, the magnetic field strength, is within a factor of not more than 10 for all components but one, component A of 2349+289. Given a large uncertainty in the model parameters suggested in the models by Miley (1980) and Slish (1963), we consider such an agreement acceptable. In the case of 2349+289, the large disagreement could be perhaps attributed to the fact that equipartition does not hold or select assumed parameters (such as, for example, the filling factor) differ significantly from the “canonical” values used by Miley (1980).

We now discuss the possibility of the existence of an energy supply at the lobes in these distant galaxies. For

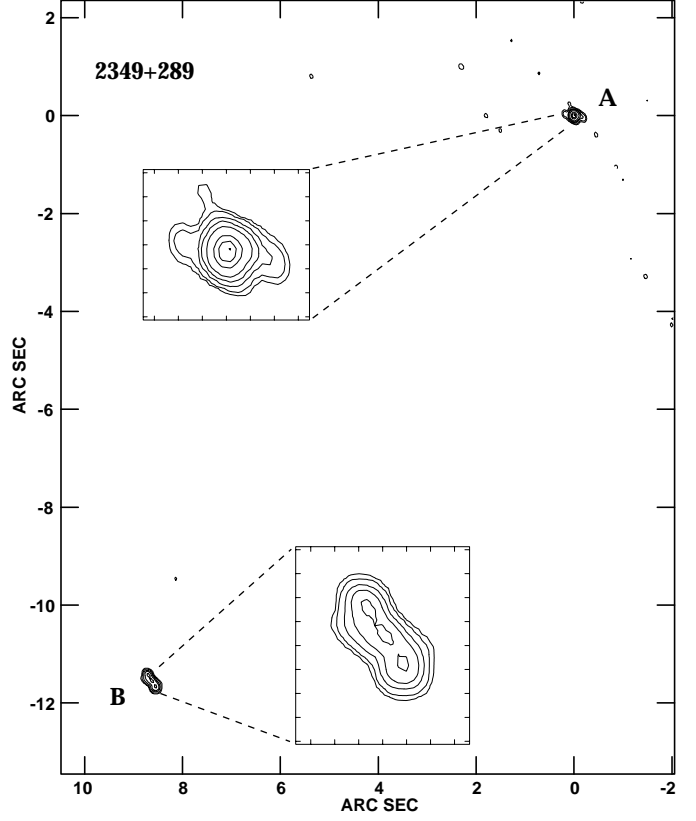


Fig. 4. Brightness distribution of the source 2349+289 at 327 MHz. Contours levels are $-2, -1, 1, 2, 5, 10, 20, 50, 75, 99\%$ of the peak flux density of 1.19 Jy/beam , beam size is $100 \times 100 \text{ mas}$. Tick separation in the insets is 100 mas .

an isotropic distribution of pitch angles, the average age of a radiating synchrotron electron is (De Young 1976)

$$t_r = 0.82 B^{1/2} (B^2 + B_r^2)^{-1} (1+z)^{-1/2} \nu_* \text{ (yr)} \quad (1)$$

where B (G) is the magnetic field strength in the source, B_r (G) is the equivalent magnetic field strength of the microwave background, ν_* (GHz) is the frequency above which an exponential drop in flux density will occur (we take $\nu_* = 4.8 \text{ GHz}$).

If we assume that there is no resupply of energy to the observed components, then their radiative lifetime can be estimated as $\tau = \frac{U_e}{L}$, where U_e is the energy of relativistic electrons associated with the component of total radio luminosity L . Both U_e and L are calculated on the assumption of energy equipartition between relativistic particles and magnetic field. The results of the calculations are listed in last two columns of Table 3.

On average, the radiative age is 1.5–2 orders of magnitude longer than the radiative lifetime estimated from the total electron energy. This is an evidence for the existence of continued energy supply to the lobes, presumably from the central object. It is likely that the injection spectrum of this energy resupply is steep in view of the overall spectra of these sources (Chambers et al. 1990).

Table 3. Physical parameters of the radio emission.

Source Name	Comp.	327 MHz Monochromatic Luminosity (10^{29} W/Hz)	Total Radio Luminosity (10^{45} erg/s)	Magnetic Field Strength (10^{-4} G)	Minimum Total Energy (10^{58} erg)	Radiative Component Lifetime τ (10^5 yr)	Electron's Age t_r (10^3 yr)
1345+245	A	4.98	4.01	33.2	3.47	2.75	0.99
	B	1.24	2.48	18.5	0.52	0.66	2.38
1809+407	A	2.58	2.28	26.6	2.44	3.40	1.51
	B	0.24	2.25	13.2	0.17	0.24	4.34
2349+289	A	6.13	5.28	78.2	1.66	1.00	0.27
	B	6.78	7.59	59.9	6.02	2.52	0.41

4. Conclusions

Three high redshift galaxies 1345+245, 1809+407 and 2349+289 from an original sample of nine objects have been imaged at an angular resolution of ~ 40 – 100 mas at 327 MHz using global VLBI data. The images allow us to identify with confidence compact components corresponding to hot spots in the VLA maps. No radio cores have been detected in our observations, which might be due to their flat or inverted spectra, or the sensitivity limitations of the observations. The morphology of these sources are simple double structures, apparently very different from those of high redshift quasars ($z > 3$) which generally possess dominant core components and weak distorted radio jet structures (Gurvits et al. 1992; Frey et al. 1997).

We have modeled the physical parameters of the three sources and found that a continuous supply of newly accelerated electrons to the lobes is required.

The asymmetric flux densities of the lobes in high redshift galaxies may be explained by the effects of mild relativistic beaming or by assuming the energy supply is asymmetric due to a clumpy or asymmetric gaseous environment in the inner part of the host galaxy. There is evidence for a substantial amount of ionized gas around high redshift radio galaxies, for example, the extremely large rotation measures (over 1000 rad m^{-2}) and large gradients in rotation measure found in the sources 0902+343 and 0647+415 (4C41.17) (Carilli et al. 1994); in addition there is extended Lyman α emission associated with the galaxies (van Ojik 1995). In principle, investigation of the polarization fraction and depolarization might provide clues on the environment in the early universe. This will require higher sensitivity VLBI observations.

Acknowledgements. Two of the co-authors, ZC and HL would like to thank the Joint Institute for VLBI in Europe (JIVE) for its hospitality and financial assistance during their visits. ZC also thanks Daniele Dallacasa for his help and support during his visit. RN and ZC are supported partly by a grant from the National Natural Science Foundation of China. The authors acknowledge support from the exchange programme of the Chinese and Dutch Academies of Sciences. This research was supported by the NWO programme on the

Early Universe. The National Radio Astronomy Observatory is a facility of the National Science Foundation operated under cooperative agreement by Associated Universities, Inc. The European VLBI Network is a joint facility of European and Chinese radio astronomy institutes funded by their national research councils. The research has made use of the NASA/IPAC Extragalactic Database NED which is operated by the Jet Propulsion Laboratory, Caltech, under contract with the National Aeronautics and Space Administration.

References

- Becker, R. H., White, R. L., & Edwards, A. L. 1991, *ApJS*, 75, 18
- Begelman, M. C., & Gioffi, D. F. 1989, *ApJ*, 345, L21
- van Breugel, W. J. M., Stanford, S. A., Spinrad, H., Stern, D., & Graham, J. R. 1998, *ApJ*, 502, 614
- Carilli, C. L., & Barthel, P. D. 1996, *Astron. Astroph. Rev.*, 7, 1
- Carilli, C. L., Owen, F. N., & Harris, D. E. 1994, *AJ*, 107, 480
- Carilli, C. L., Röttgering, H. J. A., van Ojik, R., Miley, G. K., & van Breugel, W. J. M. 1997, *ApJS*, 109, 1
- Chambers, K. C., Miley, G. K., & van Breugel, W. 1987, *Nature*, 329, 604
- Chambers, K. C., Miley, G. K., & van Breugel, W. 1988, *ApJ*, 327, L47
- Chambers, K. C., Miley, G. K., & van Breugel, W. 1990, *ApJ*, 363, 21
- Chambers, K. C., Miley, G. K. 1990, in *Evolution of the Universe of Galaxies, The Edwin Hubble Centennial Symp.*, ed. R. G. Kron (ASP), 373
- Chambers, K. C., Miley, G. K., van Breugel, W., & Huang, J.-S. 1996, *ApJS*, 106, 215
- Chambers, K. C., Miley, G. K., van Breugel, W., et al. 1996, *ApJS*, 106, 247
- Clark, B. G. 1973, *Proc. IEEE*, 61, 1242
- Cotton, W. D. 1995, in *Very Long Baseline Interferometry and the VLBA*, ed. J. A. Zensus, P. J. Diamond, & P. J. Napier, ASP Conf. Ser., 82, 189
- Diamond, P. J. 1995, in *Very Long Baseline Interferometry and the VLBA*, ed. J. A. Zensus, P. J. Diamond, & P. J. Napier, ASP Conf. Ser., 82, 227
- Dagkesamanskii, R. D., Samodurov, V. A., & Lapaev, K. A. 2000, *Astron. Rep.*, 44, 18
- Daly, R. A. 1992a, *ApJ*, 386, 43
- Daly, R. A. 1992b, *ApJ*, 399, 426

- De Young, D. S. 1976, *ARA&A*, 14, 447
- De Young, D. S. 1989, *ApJ*, 342, L59
- Dickinson, R., Tadhunter, C., Shaw, M., Clark, N., & Morganti, R. 1995, *MNRAS*, 273, L29
- Douglas, J. N., Bash, F. N., Bozayan, F. A., Torrence, G. W., & Wolfe, C. 1996, *AJ*, 111, 1945
- Evans, A. S., Sanders, D. B., Mazzarella, J. M., et al. 1996, *ApJ*, 457, 658
- Fabian 1989, *MNRAS*, 238, 41
- Frey, S., Gurvits, L. I., Kellermann, K. I., Schilizzi, R. T., & Pauliny-Toth, I. I. K. 1997, *A&A*, 325, 511
- Gurvits, L. I., Schilizzi, R. T., Miley, G. K., et al. 1997, *A&A*, 318, 11
- McCarthy, P. J., Spinrad, H., Djorgovski, S., et al. 1987a, *ApJ*, 319, L39
- McCarthy, P., van Breugel, W., Spinrad, H., & Djorgovski, S. 1987b, *ApJ*, 321, L29
- McCarthy, P. 1993, *ARA&A*, 31, 639
- Miley, G. K. 1980, *ARA&A*, 18, 165
- Miley, G. K. 1992, in *NASA/STECF Workshop on Science with the Space Telescope*, ed. P. Benvenuti, & E. Schreier, 1
- Miley, G. K., Chambers, K. C., van Breugel, W. J., & Macchetto, F. 1992, *ApJ*, 401, L69
- Pearson, T. J. 1991, *BAAS*, 23, 991
- Pentericci, L., Röttgering, H. J. A., Miley, G. K., et al. 1999, *A&A*, 341, 329
- Rees, M. J. 1989, *MNRAS*, 239, 1
- Röttgering, H., & Miley, G. K. 1996, in *The Early Universe with the VLT*, ed. J. Bergeron (Springer-Verlag), 285
- Sligh, V. I. 1963, *Nature*, 199, 682
- Tadhunter, C., & Tsvetanov, Z. 1989, *Nature*, 324, 422
- van Ojik, R. 1995, Ph.D. Thesis, Leiden Observatory
- Villar-Martin, M., Binette, L., & Fosbury, R. A. E. 1996, *A&A*, 312, 751
- Walker, R. C. 1995, in *Very Long Baseline Interferometry and the VLBA*, ed. J. A. Zensus, P. J. Diamond, & P. J. Napier, *ASP Conf. Ser.*, 247